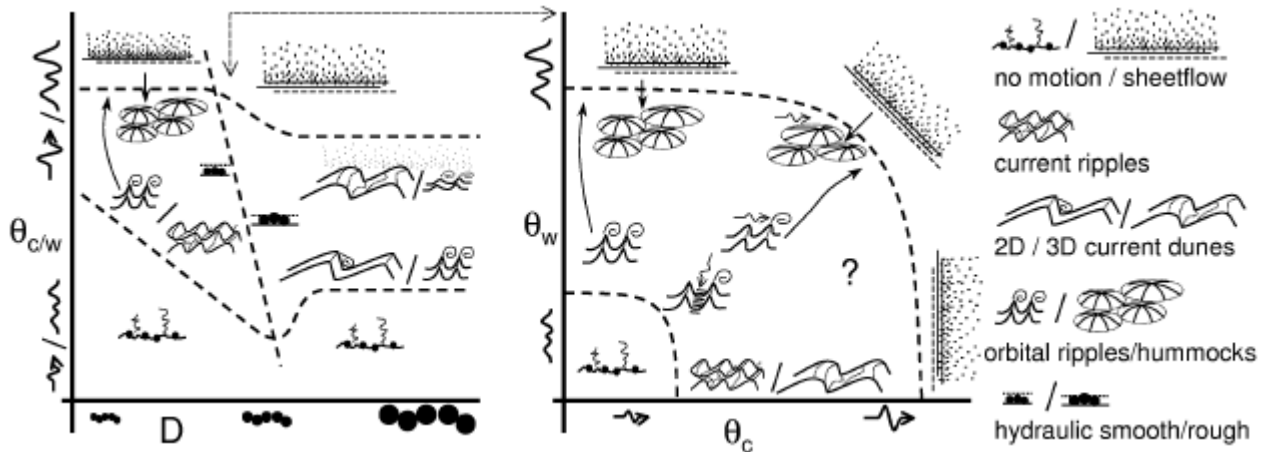


PHASE DIAGRAMS OF BED STATES IN STEADY, UNSTEADY, OSCILLATORY AND MIXED FLOWS

M.G. Kleinhans¹

(¹Utrecht University) Version: 4-1-05

PICTURE ABSTRACT



1. INTRODUCTION

In many flow or wave dominated environments the bed material is moulded in morphological features. In a hydraulic sense, basically two genetic types of forms are distinguished. First, those generated by interaction of general, changing flow or wave conditions with the bed, such as scroll bars in rivers and nearshore bars in coastal environments. Second, bedforms generated by interaction of the bed with the turbulent or orbital structures of the flow, such as current ripples, dunes and orbital ripples are formed, which may be predictable from data of appropriate hydraulic and sediment conditions. This paper is about the bedforms.

In the past decades a goal of sedimentological studies of bedforms and other bed phases was to develop empirical phase diagrams that show the regimes in which various bed states, e.g., bedforms and sheet flow, are stable. Such diagrams (e.g., Southard and Boguchwal, 1990) are used for two purposes: for assessing the likely bed states in roughly known flow conditions and sediment composition, and to reconstruct the flow conditions from known bed state or sedimentary structures in palaeo- and extraterrestrial environments. In addition, the diagrams may direct further research on bed state stability.

Phase diagrams of bed states provide a high-altitude view of current ripples, dunes, orbital ripples and other bed states and the conditions in which these occur. They are not intended to replace more detailed models (e.g. Nielsen, 1981, Van Rijn, 1993) which predict not only their emergence and disappearance but also their length or height. The phase diagrams and models are both empirically well verified, but when plotted together in the bed phase diagrams, there is a striking disagreement. Moreover, bed states in combined waves and currents are much less well mapped and understood than in currents only.

The aim of this paper is 1) to compare existing phase diagrams with existing bedform and bed state predictors, and 2) to rationalise the diagrams for currents, waves and combined flow based on more physically-based models for bed phases. First, the nondimensional variables are compared. Next, a short review is given of existing phase diagrams and bed state predictors. A set of new diagrams is then presented for currents, waves and combined flow. Rather than to fill these diagrams with many datasets, they are compared to the lines of existing, empirically well verified diagrams. Finally, the limitations and problems of the new diagrams are discussed, such as the predictability of large bedforms with poor time-adaptation in large water depths and transient conditions (e.g. floods, tides, storms).

2 PARAMETERS USED IN BEDPHASE DIAGRAMS

2.1 Choice of variables

At least eight variables are needed to characterise bed states in cohesionless sediment of uniform density, subspherical shape, approximately lognormally distributed sediment sizes, constant conditions and large

water depth (relative to grain size) (Southard and Boguchwal, 1990, Southard et al., 1990). Two or three variables are needed for the flow: water depth, velocity for currents, and orbital velocity and diameter or period for waves. The liquid is characterised by density and viscosity, which depend slightly on temperature. The sediment is characterised by grain diameter and density. By far the most natural variation is captured in the flow parameters and sediment sizes. It is attractive to use nondimensional variables for larger applicability of the diagrams.

2.2 Grain parameters

For grain size, various nondimensional parameters are in use. Within normal temperature and sediment density ranges these are so similar that they can be interchanged. The Bonnefille parameter (in Van den Berg and Van Gelder, 1993):

$$D^*=D_{50}[(Rg/v^2)]^{(1/3)} \quad (1)$$

with $R=(\rho_s-\rho)/\rho$, in which $g=9.81 \text{ m s}^{-2}$, ρ =fresh or sea water density ($1000\text{-}1025 \text{ kg m}^{-3}$), ρ_s =sediment density (2650 kg m^{-3} for quartz), D_{50} =50% median grain size and v =kinematic viscosity. The Southard and Boguchwal (1990) parameter:

$$D^*_{t10}=D_{t10}[(\rho_{t10}g(\rho_s-\rho_{t10})/\mu_{t10}^2)]^{(1/3)} \quad (2)$$

with $D_{t10}=D_{50}(\mu_{t10}/\mu)^{(2/3)}$, μ_{t10} =dynamic viscosity at 10°C , μ =dynamic viscosity, and ρ_{t10} =density of water at 10°C . The emphasis on temperature is relevant for the transition of current ripples to dunes. The Dingle and Inman (1976) parameter, which is a cube root version of the above:

$$D^*=D_{50}^3 Rg/v^2 \quad (3)$$

The Grant and Madsen (1982) parameter:

$$S^*=D_{50}^{1.5}(Rg)^{0.5}/(4v) \quad (4)$$

which differs precisely a factor of 4 from the particle Reynolds number (e.g. Parker in prep.):

$$R_{ep}=D_{50}^{1.5}(Rg)^{0.5}/(v) \quad (5)$$

while $R_{ep}=D^*_{1.5}$. The settling velocity w_s of sediment is directly related to the grain size (e.g. Soulsby, 1997).

2.3 Flow parameters

Three types of flow parameters are commonly used: based on current velocity, shear stress (including form drag) and grain shear stress (only skin friction). The shear stress is given by $\tau_c=\rho g h i$ or $\tau_c=\rho u^*$, where h =water depth (corrected for wall roughness for narrow channels), i =energy slope and u^* =shear velocity. Inserting the White-Colebrook friction law for hydraulic rough conditions, shear stress is given by:

$$\tau_c=(1/8)\rho f_c u^2 \quad (6a)$$

$$f_c=0.24(\log 12h/k_s)^{-2} \quad (6b)$$

where u =depth-averaged current velocity and k_s =hydraulic (Nikuradse) roughness length. Following Van Rijn (1984), the grain shear stress is estimated by equating the k_s to a representative grain size, e.g. $2.5D_{50}$, D_{90} , or $3D_{90}$. Alternative friction laws are available and represent another choice to be made.

Three types of nondimensional flow parameters are commonly used: based on orbital velocity, wave mobility and wave shear. The orbital velocity u_{orb} , orbital diameter A_{orb} and wave period T are related as:

$$A_{orb}=(u_{orb}T)/2\pi \quad (7)$$

Obviously an important choice has to be made here: which waves are representative for the wave field. Commonly used parameters are the rms, the mean of the 1/3 or 1/10 largest waves computed from the time domain, or the significant wave height and peak period computed from the frequency domain (see discussion).

The wave mobility parameter is:

$$\psi=u_{orb}^2/(RgD_{50}) \quad (8)$$

The wave grain shear stress is computed with the combination of:

$$\tau_w=(1/2)\rho f_w u_{orb}^2 \quad (9a)$$

$$f_w=\exp[5.213(2.5D_{50}/A_{orb})^{0.194}-5.977] \quad (9b)$$

according to Swart (in Soulsby, 1997) with $A_{orb}=(u_{orb}T)/2\pi$. Alternative roughness formulations are available and represent another choice to be made.

The shear stress in combined currents and waves is still debated. Two common forms are by Bijker:

$$\tau_{cw}=\tau_c+0.5\tau_w \quad (10)$$

and by Soulsby (1997):

$$\tau_{cw}=\tau_c\{1+1.2[\tau_w/(\tau_c+\tau_w)]^{3.2}\} \quad (11)$$

in which τ_{cw} = effective grain-related shear stress of the current affected by waves. The maximum shear stress due to waves plus current must exceed the critical shear stress for motion in order for sediment motion to occur (Soulsby, 1997) and is computed as:

$$\tau_{cwmax}=[\tau_w^2+\tau_{cw}^2]^{0.5} \quad (12)$$

assuming the wave propagation direction perpendicular to currents. All shear stress parameters are nondimensionalised as the Shields parameter:

$$\theta=\tau/[(\rho_s-\rho)gD_{50}] \quad (13)$$

so that $\theta=(1/2)f_w\psi$.

Two other parameters are necessary to describe the flow: the Froude number which defines the transition between subcritical and supercritical flow (relevant for, e.g., intertidal areas) at about $Fr=0.7-1$ as:

$$Fr=u/(gh)^{0.5} \quad (14)$$

and the Reynolds number, which defines the transition between hydraulic smooth and rough conditions for which grains protrude into the flow above the laminar sublayer δ at $Re^*=11.63$ (3.5 to 70) as:

$$Re^*=u*D/\nu \quad (15)$$

3. REVIEW OF BED STATE CRITERIA

3.1 Bed state definitions

Bed state descriptions are numerous, commonly ambiguous, often confusing and sometimes incomplete. Tentative bed state definitions herein are taken from Ashley (1990) and Swift et al. (1983) (table 1). Eventually bedforms will have to be defined in an objective way. Following Ashley (1990), bed states should be defined descriptively rather than genetically, but it is impractical to avoid terminology such as current or wave ripple. Moreover, the observation of a bed state such as plane bed depends on the range and accuracy of echo sounding instruments. A very accurate instrument may detect ripples of small height where a less accurate instrument (or casual observer) finds a plane bed, or the wave length of the bedform may be much larger than the scanning range of the instrument. A further complication is superposition of bed states (Bridge, 1981).

Table 1. *Tentative bed state definitions.*

Bed state name	Tentative bed state definition
lower stage plane bed	plane bed with maximum roughness lengths of $O(D_{50})$ for a plot of size $O(1m^2)$ (excluding biogenic features), no or marginal motion of sediment
upper stage plane bed	plane bed with maximum roughness lengths of $O(D_{50})$ for a plot of size $O(1m^2)$ with much sediment suspension and a sediment layer of several D_{50} thick in motion by the flow, associated with large orbital and/or current flow velocities but subcritical flow ($Fr<0.8$), containing parallel lamination
upper flow regime, antidunes	plane or undulating bed with undulations moving against the flow direction, associated with critical flow (plane bed, $Fr\sim 0.84$) or supercritical flow ($Fr>1$)
current ripples	linguoid bedforms with maximum length $O(0.4m)$ and height $O(0.02m)$, equilibrium dimensions are independent of flow conditions, non-equilibrium form may be straight-crested, associated with hydraulic smooth flow ($Re^*<11.6$) or $D_{50}<0.7$ mm, containing small-scale cross-stratification
current dunes	approximately triangular cross-sections but often convex-upwards stoss sides, lee side commonly at angle of repose and vortex shedding, observed height and length from smaller than current ripple sizes to $O(10m)$ high and $O(100m)$ long, equilibrium dimensions depend on flow conditions, e.g. dune height is 0.15-0.35 of water depth, associated with hydraulic rough flow ($Re^*>11.6$) or $D_{50}>0.7$ mm, containing large-scale cross-stratification,
3D vs 2D dunes	2D dunes are straight or wavy-crested with small variations in dune top height and trough scour depth, whereas 3D dunes are lunate, cusped or linguoid with much variation in dune top height and trough scour depth, transition 2D to 3D is associated with sediment mobility or, alternatively, 2D dunes are not in equilibrium with the flow
wave ripples	concave-upwards two-sided (or more) slip faces, maybe straight-crested in sand of $D_{50}>0.5$ mm and calm conditions but otherwise highly irregular, when sharp-crested with top angles approximating the angle of repose, there is also vortex shedding from the tops

hummocks	convex-upwards semi-spherical forms in an irregular spatial pattern, observed heights $O(0.1m)$ and lengths $O(1-10m)$, with much sediment suspension but no strong vortex shedding, associated with large orbital flows possibly combined with small currents but origin unclear, containing Hummocky Cross-Stratification (HCS): semi-parallel lamination in undulating bands
mixed flow ripples	bedforms with characteristics of both flow and current bedforms, e.g., weak current action on wave bedforms in following or opposing current causes skewness in the current direction, perpendicular small currents and waves give current ripples in the troughs of wave ripples, weak wave action on current bedforms causes rounding, equal current and wave action commonly causes irregular bedforms
long wave ripples	wave ripples larger than, and subimposed on commonly found wave ripples while both are active and stable, origin unclear but possibly similar to skewed hummocks
megaripples	in currents probably equal to dunes, in waves origin unclear but possibly similar to skewed hummocks

3.2 Current bed states

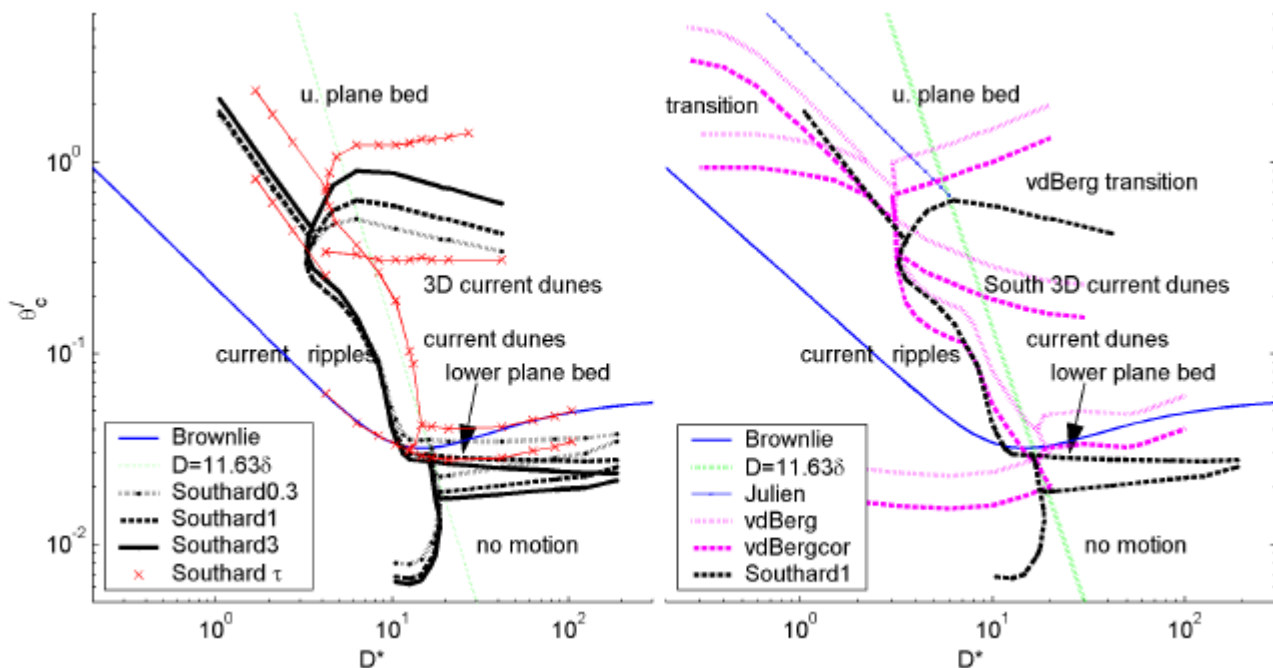


Figure 1 Current bedform stability diagrams of Van den Berg and Van Gelder (1993) and Southard and Boguchwal (1990). The BG is also given adjusted for using $2.5D_{50}$ rather than $3D_{90}$ as grain roughness. The SB is given for three water depths and in the total shear stress version. The line between dunes and transition in BG is for flume experiments only. See text and Figure 2 for the upper stage plane bed (Julien) and hydraulic smooth/rough criteria ($D=11.63d$).

For steady currents highly detailed and well verified diagrams are available. Simon and Richardson presented one of the best known diagrams with grain size and flow velocity, based on flume experiments. Its fatal flaw is that bed states in critical and supercritical flow are included, which depends on the Froude number. Allen (1984) provides an overview of early diagrams, and presents his own based on total bed shear stress (including form drag) and grain size. Southard and Boguchwal (1990) (SB) presented an authoritative set of empirical diagrams with nondimensional variables of flow velocity and grain size, accounting for temperature (viscosity) and gravity effects, and one diagram with nondimensional shear stress (including form drag) and grain size. The diagrams were drawn for various water depths and have fields for lower stage plane bed (LPB), current ripples (CR), two- and three-dimensional dunes (2D/3D CD), various transitional fields and upper stage plane bed (UPB). One of their diagrams was based on total shear stress which has the same flaw as the Simons and Richardson diagram. Van den Berg and Van Gelder (1993) (BG) collapsed these diagrams in one diagram by removing the water depth effect caused by form drag. They introduced nondimensional grain shear stress (Shields parameter) rather than flow velocity or total shear stress, following the concept of Van Rijn (1984). Carling (1999) extended existing diagrams into the grain size range of coarse gravels, while Kleinhans et al. (2002) demonstrated effects of mixtures of sand and gravel on bedform type.

The diagrams of SB and BG are directly comparable assuming a grain roughness of $2.5D_{50}$, correcting the BG for the adjusted roughness ($2.5D_{50}$ rather than $3D_{90}$) and calculating grain shear stress for SB for three water depths (Figure 1). The $2.5D_{50}$ is chosen here for the practical reason that for many coastal datasets only the D_{50} is given, and works well for sediment transport computations (Nielsen, 1992). As expected, various parts of the diagrams based on velocity and grain shear stress are similar, notably the transition between ripples and dunes. The diagram based on total shear differs much from the others and is further ignored. There is strong disagreement about the onset of (subcritical) upper stage plane bed (UPB) and incipient motion.

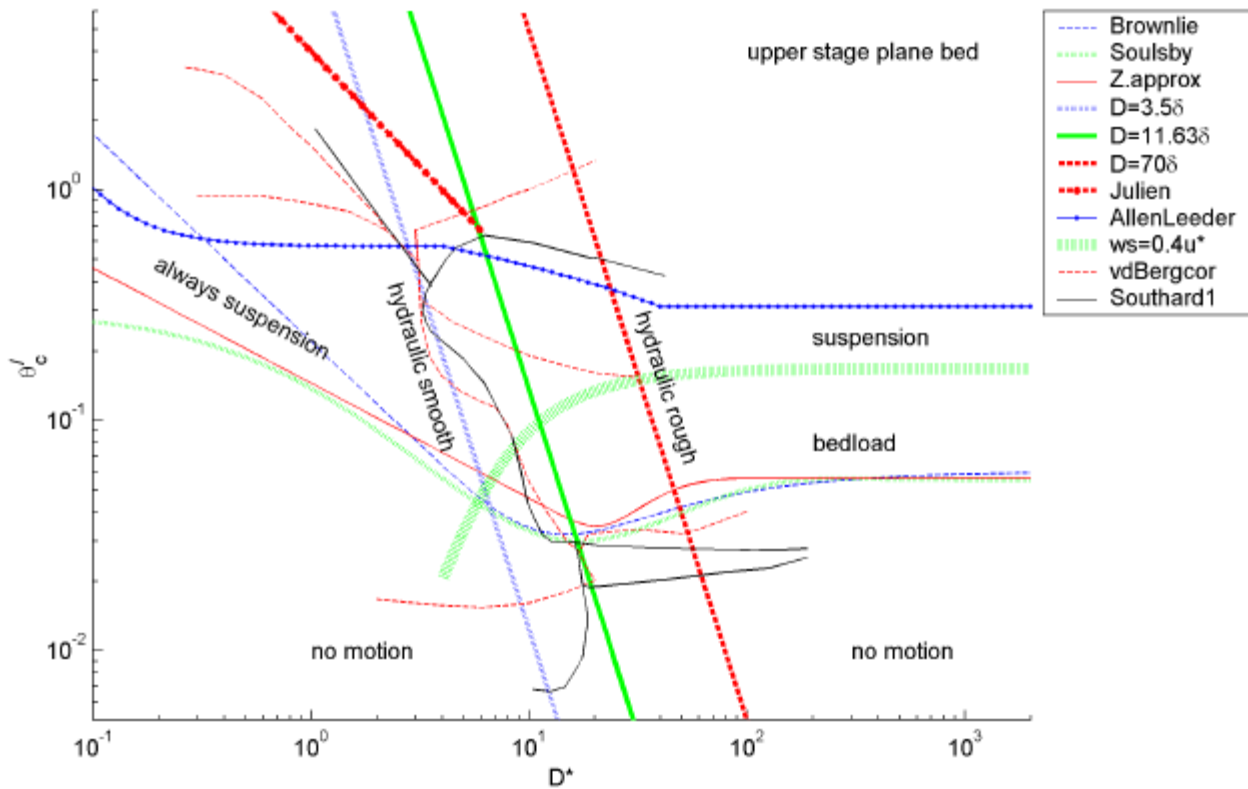


Figure 2 Current criteria for incipient motion (Brownlie, Soulsby, Zanke approximation), suspension, upper stage plane bed and hydraulic rough/smooth flow transitions.

Incipient motion in currents has first been studied in detail by Shields (1936, in Soulsby, 1997). A highly detailed empirical test of the Shields criterion, including various definitions of incipient motion, is given by Buffington and Montgomery (1997, 1998). A reasonably good physical model replacing the empirical Shields criterion was developed by Wiberg and Smith (1987), while a better model was developed independently by Zanke (2003) (Figure 2), who included cohesion by water and clean sand or silt, drag and lift forces and the effect of turbulence and water depth. Predictors for current bedforms are not discussed here (see Wilbers 2004 for an overview). The transition between current ripples and dunes coincides more or less with the transition between hydraulic rough and smooth flow (Allen and Leeder 1980).

The transition to (subcritical) upper regime plane bed conditions in currents in fine sand was studied by Julien and Raslan (1998) for both hydraulic smooth and rough beds. Allen and Leeder (1980) modified a Bagnold criterion for UPB for both ripple and dune conditions, which coincides with the UPB criterion of BG. However, contrary to the stability diagrams, the Allen-Leeder criterion is independent of grain size in the hydraulic smooth and rough ranges.

3.3 Wave bed states

For waves not many diagrams are available. The best known is by Allen (1984) which is based on maximum orbital velocity and grain size. There are only three stability fields: upper stage plane bed, wave ripples and lower stage plane bed (Figure 3). Since then, the behaviour of wave ripples and the transition to sheetflow has been described in empirical predictors rather than diagrams (see below) in the coastal engineering literature. In those functions, a bedform of sedimentological significance has been largely neglected however: the hummock with its associated hummocky cross-stratification (HCS). Only Southard et al. (1990)

presented empirical phase diagrams for wave ripples, hummocks and sheet flow from oscillatory flow tunnel data for various grain sizes.

Incipient motion under waves has been compared to that under currents by Sternberg and Larsen (1975) Soulsby (1997) and others. Green (1999) addressed the problem of which wave parameter is representative for the wave field, and found that various combinations of wave height, period, shear stress and wave-current interaction formulations collapsed the data onto the Shields criterion..

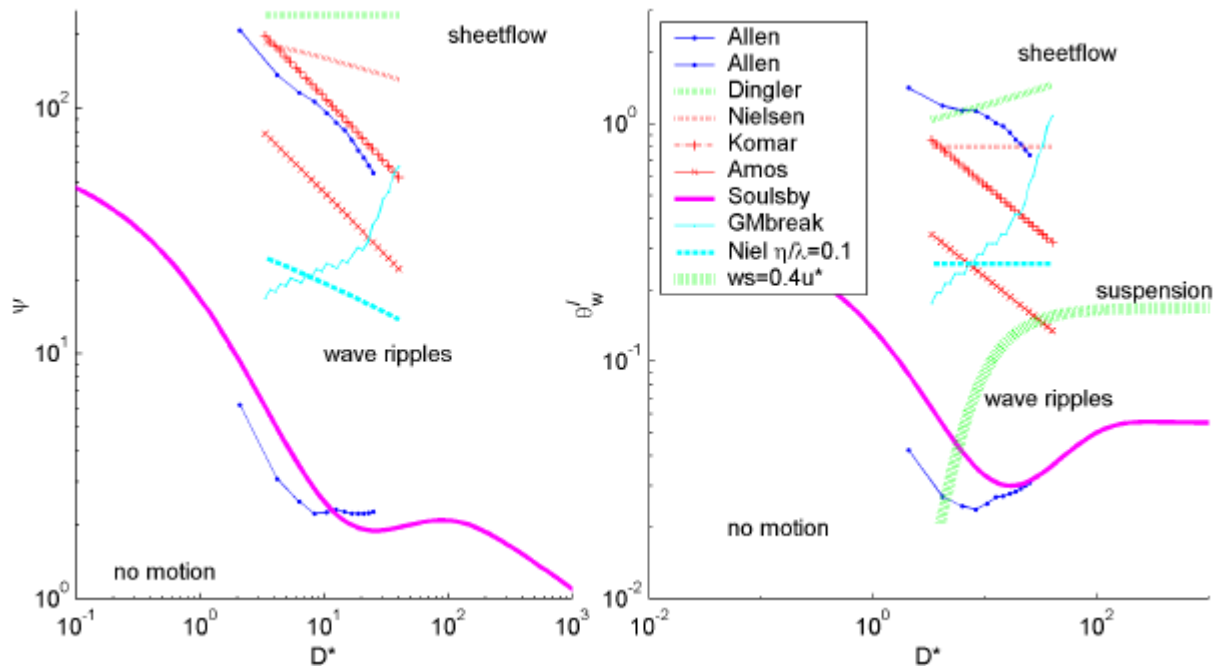


Figure 3 Wave bedform stability diagram and criteria plotted for wave mobility (left) and Shields parameter (right). To indicate when wave ripples become less high with increasing conditions, the Grant and Madsen (1982) break-off point and the point at which the Nielsen (1981) ripple steepness is 0.1 are indicated.

There are many predictors for orbital ripple dimensions (see Grasmeijer and Kleinhans, 2004, for an overview). These are commonly based on grain size and a nondimensional wave mobility parameter or a nondimensional wave grain shear stress. Commonly two ranges are identified: a lower mobility range in which the steepness of ripples is limited by the angle of repose only, and in which ripple length scales with orbital diameter and grain size, and a higher mobility ('break off') range in which the ripples are flattened in the transition to sheet flow conditions and scale with grain size. In effect, these ripple predictors contain a sheet flow criterion and a diffuse transition, the break off, to 'much' suspension (Figure 3).

Empirical predictors for sheet flow under waves and combined flows have been presented by Komar and Miller (1975b), Amos et al. (1996), Li and Amos (1999) and others. The later also addressed the choice of the representative wave parameter. When these criteria are extrapolated to smaller and larger grain sizes, they predict inconsistently (Figure 3). For coarse gravel, the sheetflow onset is predicted at initial motion, whereas for fine sand and silt the sheetflow is at very large Shields numbers. For the criteria and bedform predictors assuming a constant wave mobility number for the sheet flow transition the inconsistency is similar. The Allen-Leeder criterion was also tested for waves and is grain-size independent, but was ignored in engineering literature.

3.4 Combined flow bed states

Surprisingly, there are more diagrams for combined currents and waves than for waves only. The first is by Arnott and Southard (1990) (AS), which is based on oscillatory and unidirectional velocity corrected for temperature effects. The diagram is based on oscillatory flow tunnel data with sinusoidal, regular flow and very fine sand. It explicitly addresses the transition from hummocks to current dunes. Myrow and Southard (1991) extrapolated AS to larger current velocities. Amos et al. (1988, 1996) present diagrams based on the nondimensional grain shear stress for currents and waves. The bedform observations are all from the Nova Scotia shelf at 20-50 m water depth. Bed states include mixed wave-current ripples, hummocks and oriented hummocks (modified by currents), and sheet flow. Wave ripples occurred up to the sheetflow condition in rising storm, but in waning storm hummocks emerged and remained active in smaller mobilities while wave ripples remained absent. This asymmetry was also found by Li and Amos (1999a,b). The association of

hummocks with waning storm suggests a high preservation potential, which agrees with the frequent occurrence of hummocks on sonar images and hummocky cross-stratification in ancient and modern shelf deposits. Van Rijn (1993) presented a comparable diagram based on laboratory experiments in a shallow wave-current tank. The AS and Amos diagrams are directly compared assuming a grain roughness of $2.5D_{50}$ (Figure 4).

The addition of wave asymmetry, irregularity or a steady current to orbital flow leads to sheet flow at smaller Shields numbers. Ribberink (1995) experimentally studied the transition to sheetflow in combined flow in 0.21 mm sand. The orbital flow was regular asymmetric. For following currents sheetflow is attained at much smaller Shields numbers than for opposing currents. In regular sinusoidal flows sheetflow is difficult to attain at all compared to irregular orbital flow (Ribberink and Al-Salem 1994). This is confirmed in Arnott and Southard (1990) who used regular sinusoidal flow. Wilson et al. (1995) found with comparable experiments that in asymmetric flow sheetflow is attained at a much smaller Shields number than in symmetric flow.

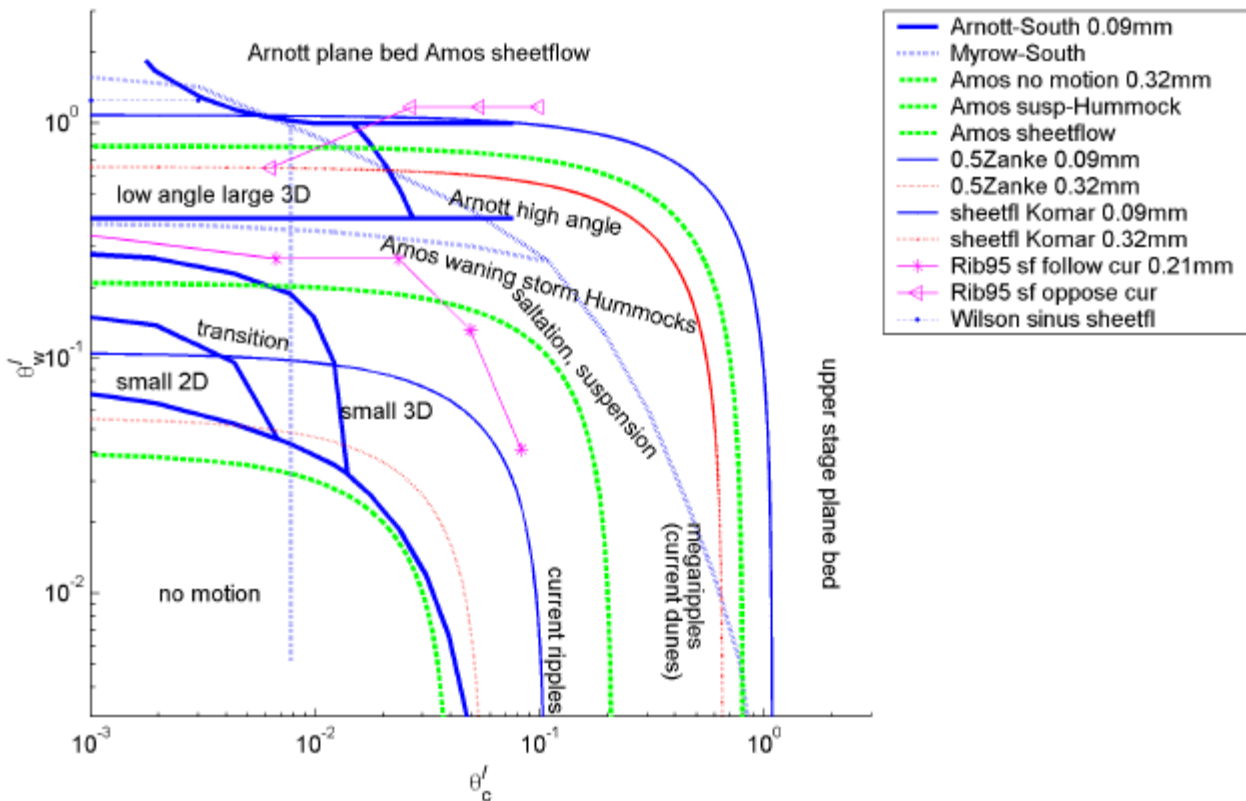


Figure 4 Combined flow bed state diagrams and criteria for various grain sizes. The data of Ribberink (1995) indicate the effect of following or opposing currents on the sheetflow transition.

4 NEW PHASE DIAGRAMS BASED ON RATIONAL CRITERIA

4.1 New diagram for currents

For currents, four bed state stability fields are defined by three physically-based functions (Figure 5): incipient motion given by the modified Zanke model, the transition between hydraulic smooth and rough conditions at $D=6\delta$ (or $D\sim 0.7$ mm) and the transition to UPB modified from Allen-Leeder. Ripples and dunes are gradually washed out nearer to the UPB. The modified Zanke model is approximated for its standard angle of repose, turbulence condition and large h/D as:

$$\theta_{cr}=0.5[0.145D^{*-0.5} + 0.045 10^{(X)}] \quad (16)$$

in which $X=1100D^{*(-9/4)}$. The factor 0.5 is the modification, which agrees with the BG and SB diagrams as well as with the low transport criteria commonly used in the gravel bed river literature. The modified Allen-Leeder criterion is given by:

$$\theta_{sh}=KC_0 \tan \psi \quad (17)$$

in which $C_0=0.6$ is bed surface sediment concentration (1-porosity), $\tan\psi$ =angle of repose, which is 0.95 for $D<0.2$ mm and 0.52 for $D>2$ mm and loglinearly decreasing from $D=0.2$ mm to $D=2$ mm, K =cohesion of the water-sand system (quartz assumed), approximated by Zanke (2003) as:

$$K=1+3 \cdot 10^{-8}/[(\rho_s-\rho)D^2] \quad (18)$$

In increasing shear stress, bedforms become more three-dimensional and eventually are washed out. Given enough time, current ripples always become 3D (Baas 1994). The very gradual transition between 2D and 3D current dunes is possibly related to the gradual onset of suspension, here arbitrarily defined at $w_s=\kappa u^*$. This would not explain the flattening of the current ripples, however. An alternative explanation is that sheetflow is attained at the ripple or dune tops while not yet on their stoss sides at lower Shields values (Bridge, 1981, 1982, Davies, 1982). Assuming a steepness of the bedform and the enhanced shear stress predictor for wave ripples by Nielsen (1984):

$$\theta_{cr}=\theta/[1-\pi(\lambda/\eta)] \quad (19)$$

it was calculated when the modified Allen-Leeder criterion was exceeded by the enhanced grain shear stress based on the steepest bedforms (Figure 5). For ripples, $\lambda/\eta=8.2$ was assumed (Baas 1999) and for dunes the steepness was computed from $\eta_{max}=0.16\lambda^{0.84}$ (Ashley 1990) assuming $\lambda=5$ m. The choices are somewhat arbitrary but transition is very gradual anyway.

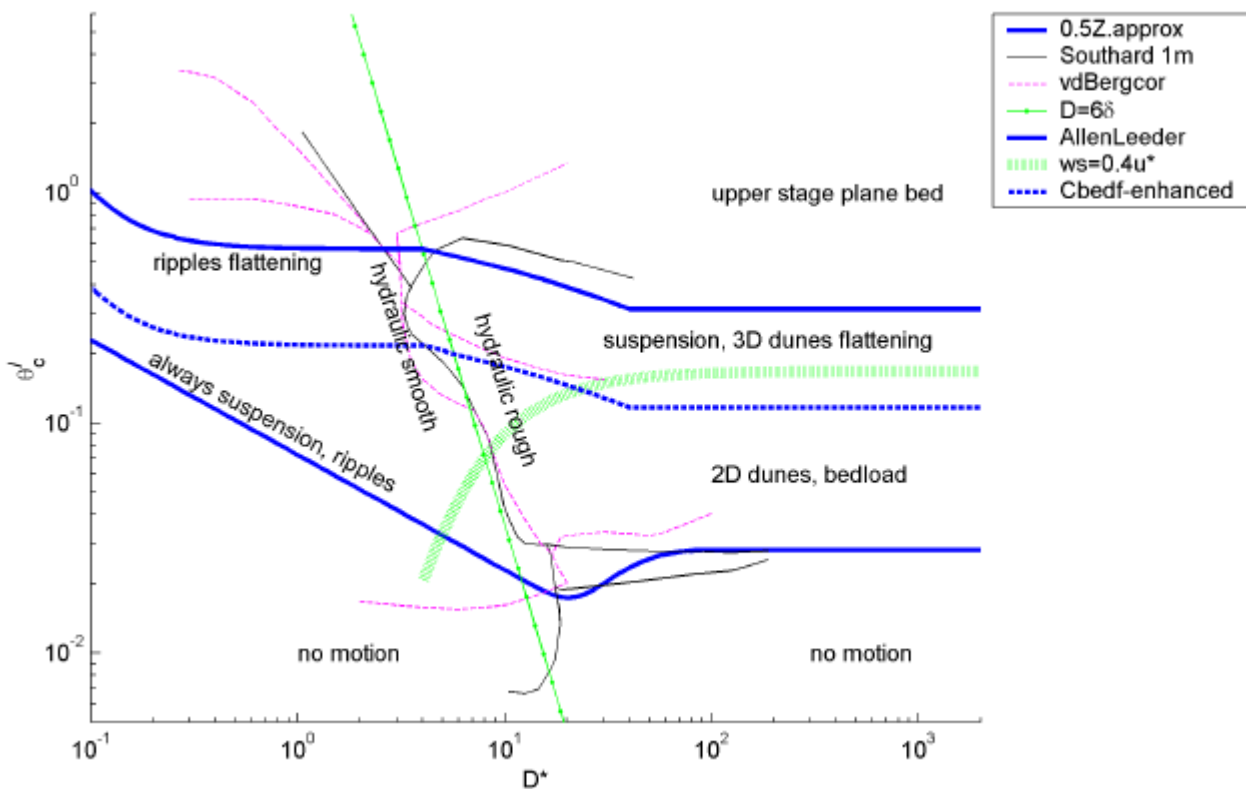


Figure 5 New current bed state diagram based on rational criteria. The Allen-Leeder criterion for UPB is modified here with the cohesion effect of Zanke (2003).

4.2 New diagram for waves

For waves, three bed state stability fields and a number of transient bed states are defined by two functions (Figure 6): incipient motion given by the modified Zanke model and the transition to UPB or sheetflow modified from Allen-Leeder, both exactly the same as for currents. The Zanke model for currents is applicable to waves, because the turbulent flow characteristics very near to the bed in the wave boundary layer are similar to that in the current boundary layer. Only the flow very near to the bed is relevant for incipient motion, which is expected to be in equilibrium much faster than the wave period. The bed states UPB and sheetflow in waves are assumed to be similar, but this is not certain for currents. The transition between hydraulic smooth and rough conditions probably has no meaning for waves except for incipient motion as reflected by the dip in the Zanke model.

The Allen-Leeder sheetflow criterion can in principle be modified for sinusoidal or asymmetrical and monochromatic or irregular waves by calculating the effective Shields parameter from different flow

parameters (see discussion). Given the existence of natural steep, sharp-crested wave ripples in coarse gravel and cobbles it is unlikely that the sheetflow criteria of Komar and Amos can be extrapolated to coarser (and finer) sediments. Rather, it corroborates the modified Allen-Leeder criterion. Assuming the wave ripple steepness predictor of Nielsen (1981) and Nielsens equation for enhanced shear stress on ripple tops, it was calculated when the modified Allen-Leeder criterion was exceeded by the enhanced grain shear stress. This line agrees well with the break-off transition where ripples are flattened in increasing shear stress. When the wave ripple stability field is entered from the sheetflow regime, hummocks are predicted. Southard et al. (1990) experimentally found hummocks to occur under purely oscillatory flow as well as under combined flow with wave dominance.

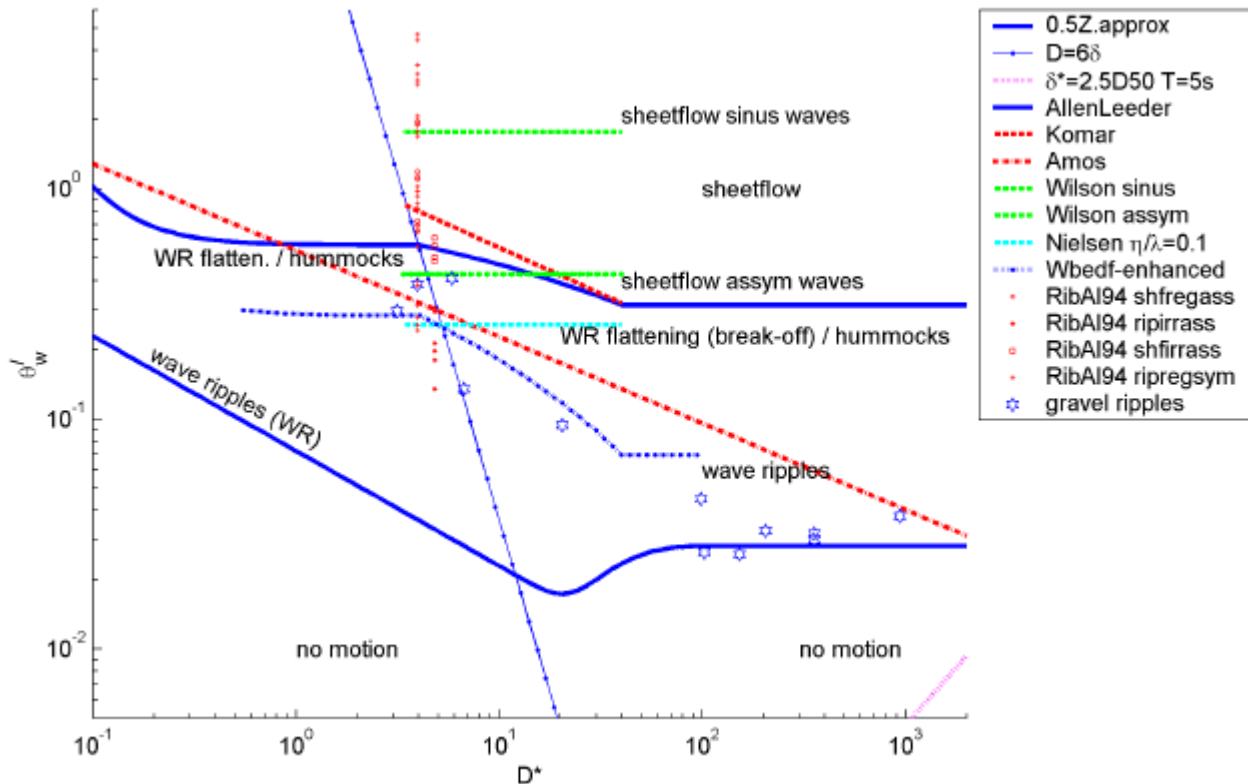


Figure 6 New waves bed state diagram based on rational criteria. The effect of wave asymmetry according to Wilson is shown, as well as the data of Ribberink and Al-Salem (1994) on which this effect was tested by Wilson. The Shields values for which the concurrent ripple-enhanced Shields values exceed the modified Allen-Leeder sheetflow criterion are based on the Nielsen wave ripple steepness predictor. Data of sharp wave ripples in $D < 40$ mm sediment (Forbes and Boyd 19??, Arduin et al. 19??) indicate that the sheetflow criteria of Komar and Amos cannot be extrapolated.

The transition between 2D and 3D wave ripples is not well understood. Many observations suggest that ripples are commonly 2D (straight-crested) for $D > 0.4$ mm, but both 2D and 3D for $D < 0.4$ mm. Doucette (pers. comm.) found that a combination of grain size and orbital diameter separates 2D from 3D ripples for $D < 0.4$ mm. The proximity of the 0.4 mm limit to that for current ripples (0.7 mm) suggests a relation with the hydraulic smooth/rough transition within the wave boundary layer as in currents but this is speculative.

4.3 New diagram for combined flows

For combined waves and currents, three bed state stability fields and a number of transient bed states are defined by two functions (Figure 7): incipient motion given by the modified Zanke model and the transition to UPB or sheetflow modified from Allen-Leeder. The diagram is essentially three-dimensional, but the grain size influence is limited compared to that of wave and current shear and the diagram is plotted for an average of $D = 0.21$ mm. Regions of dominant wave or current or combined flows are indicated by the ratios of wave and current Shields values. Whether waves or currents have any effect at all is assessed by the ratios of wave or current Shields values with the critical current or wave Shields values, respectively. A factor of 5 or 1/5 for these ratios appears to separate the various bed states rather well, although this is an arbitrary choice for a transition.

According to wave-current interaction models, the criteria are exceeded at slightly smaller Shields values, but compared to the uncertainty and transitional nature of the criteria the interaction can safely be neglected

for the calculating the Shields parameter. This is not the case, however, for the bedform type. In waves opposing or following currents, the bedforms become skewed and high-angled on the current lee side. In waves perpendicular to currents, two bedform types may be superimposed (current ripples or dunes and wave ripples or hummocks). Moreover, wave asymmetry and irregularity cause different effective mobilities (see discussion). The high-altitude view of the diagram does not separate between these different bedform morphologies, yet has predictive power for the more general transitions. The diagrams of Arnott-Southard and Myrow-Southard suggest a much larger effect of wave-current interaction. This may well be, however, an artefact as their diagrams were drawn in linear velocity space based on limited data and using simple curves.

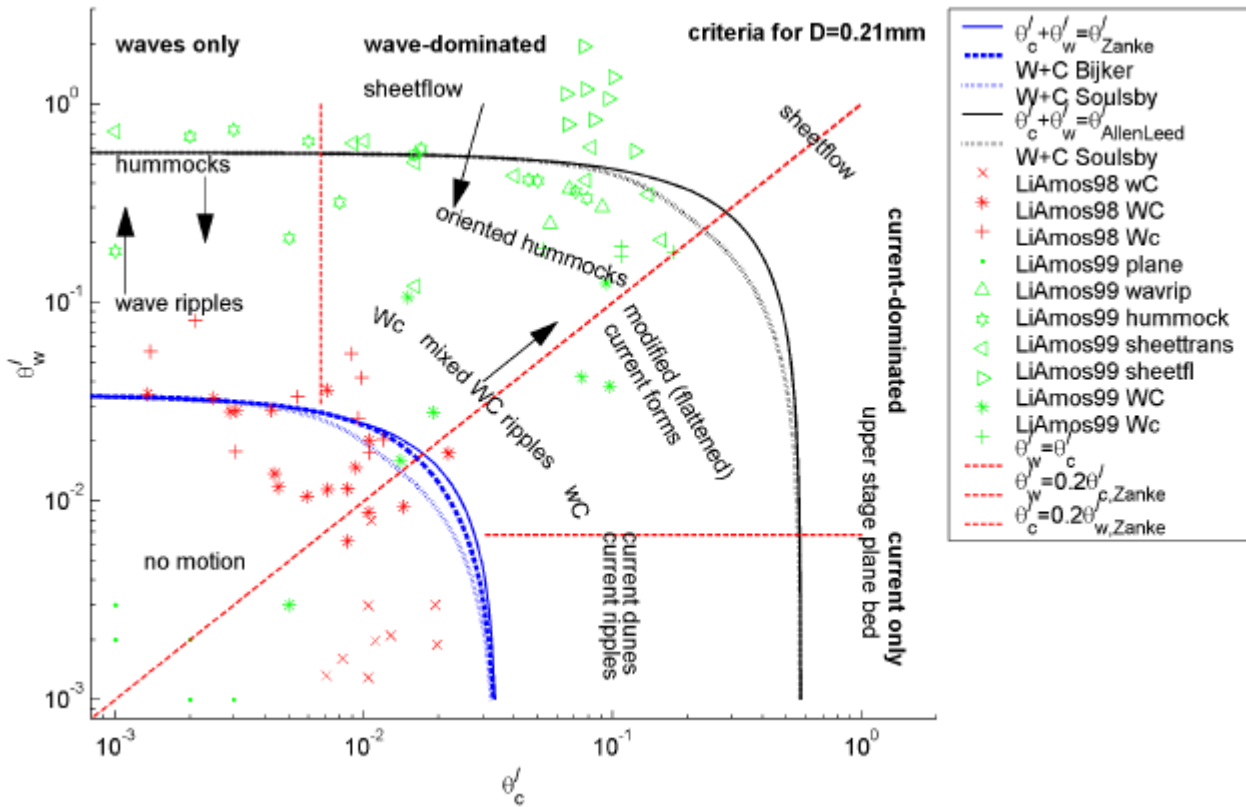


Figure 7 New combined flow bed state diagram based on rational criteria for beginning of motion and sheetflow/UPB (here plotted for $D=0.21$ mm). The effect of wave-current interaction is very small. Regions of wave or current dominance are indicated by given ratios of wave and current Shields values. The arrows indicate for which initial conditions the bed states are valid (see text). Mixed wave-current ripples vary much in morphology depending partly on the angle between currents and waves. Regions for wave domination, current domination and waves plus current or current plus waves are indicated.

4.4 Normalisation to remove grain size effects in the combined flow diagram

The new diagram for combined flow can only be plotted for one grain size because the criteria vary with grain size. A mobility parameter M was devised which postulates the Shields criterion at $M_c + M_w = \alpha$ and the sheetflow at $M_c + M_w = \beta$:

$$M = [(\theta_i - \theta_{cr}) / (\theta_{sh} - \theta_{cr})] (\beta - \alpha) + \alpha \quad (20)$$

in which θ_i = Shields parameter of an observation. The parameters $\alpha=0.05$ and $\beta=1$ are here conveniently chosen approximating the Shields criteria. The effect of normalisation is that observations plot in the appropriate stability field independently of grain size, which allows the direct comparison of the data for $0.03 < D < 40$ mm (Figure 8). This parameter set provides a framework within which other sheetflow or incipient motion criteria can be tested as well. Again, some of the Li and Amos (1998) data plots below incipient motion, but otherwise the new criteria clearly have predictive capabilities given the ranges of grain size and conditions.

5 DISCUSSION

5.1 Status of boundaries

The status of the boundaries between bed states varies. Some transitions are sharp or diffuse (ontology), and some are well established or speculative (epistemology). Four classes are distinguished following Southard and Boguchwal (Table 2). For ontology these are abrupt (20% data spread), transition (factor of 2 spread), gradual (factor of >3 spread) and overlap. For epistemology these are established in earlier research, competitive with comparable theories, hypothetical (with theory) and speculative (without theory).

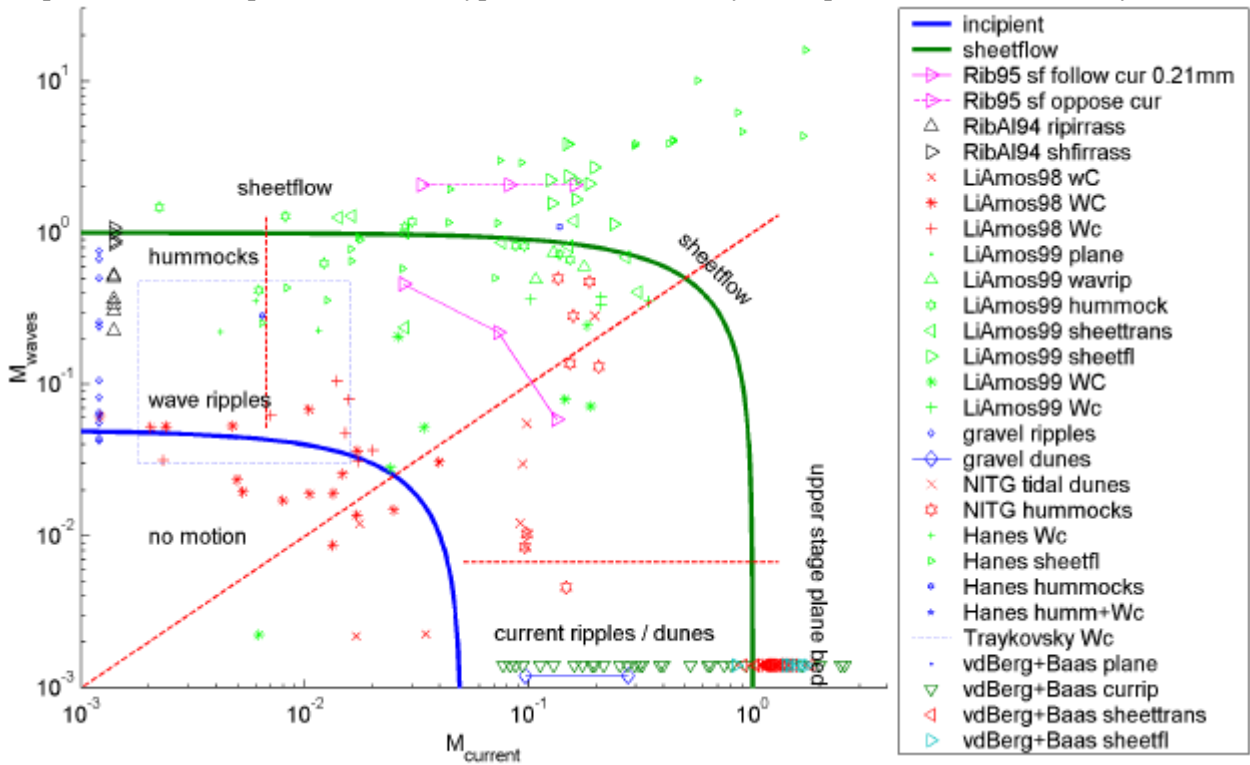


Figure 8 Normalised bed state diagram based on rational criteria for beginning of motion and sheetflow/UPB, normalised to remove the grain size influence on the criteria. Gravel ripples are same as in Figure 6. Current gravel dunes are from field data of Dinehart (1992) in $D=32$ mm. The dotted box indicates the position of the Traykovski et al. data which contains incipient motion (bottom), 2D and 3D wave ripples modified by a small current. Experimental current ripple data in silt and sands are of Van den Berg and Van Gelder (1993), and Baas (1994, 1999), Baas and de Koning (1995).

Table 2 Status of the transitions between bed states.

flow type	transition	ontological status	epistemological status
currents	beginning of motion	abrupt	established
	suspension	gradual	competitive
	bedform flattening	gradual	hypothetical
	2D/3D dunes	gradual	speculative
	hydraulic smooth/rough	abrupt	established
	UPB, sheetflow	transition	competitive
waves	beginning of motion	transition	competitive
	2D/3D orbital ripples hummocks	overlap overlap with orbital ripples (depending on history)	speculative hypothetical
	bedform flattening sheetflow	gradual transition	competitive hypothetical
mixed	beginning of motion	transition	hypothetical (wc-interaction)
	wave/current dominated oriented hummocks	overlap (depends on wc-angle) overlap with orbital ripples (depending on history)	hypothetical hypothetical
	sheetflow	overlap (depends on wc-angle)	hypothetical

5.2 Choice of wave parameter

Various authors favour the mean of 1/3 highest waves for the computation of orbital velocity (e.g. Green, 1999, Amos et al., 1988), while others have better results with the 1/10 highest waves (Amos et al., 1996, O'Donoghue, pers. comm.). The latter information is, unfortunately, not always available. The effect of wave asymmetry and superimposed small currents is that sheetflow is attained at lower shear stress. Apparently the bedforms need more time than a few waveperiods to build up, and are destroyed by the very few largest waves, which likely are also more asymmetric than smaller waves. A parameter describing these largest flow variations (maybe normalised to the 1/3 or significant flow) is probably needed to discriminate between bed states. Also the precise definition of plane bed or sheetflow causes variation. For a rotary sonar the natural seabed may already be plane whereas a laboratory laser profiler might still find ripples.

Natural waves are not monochromatic, and the shape of the spectrum varies with conditions (e.g. rising or waning storm, swell). Moreover, the small waves of the spectrum decay faster with water depth than the large waves. For deep shelf environments the spectrum of near-bed flow therefore deviates much from that of surface elevation (Soulsby, 1987). Computations of the 1/3 largest near-bed flows from surface wave records or near-bed flow recordings give different results and possibly different bedforms, which is important when plotting data from different sources in one diagram. The effect of different choices of water depth, bed profiling accuracy and wave parameters in wave-related nondimensional shear stress will be quantified in a longer future paper.

5.3 Hysteresis and history effects: the tardy reaction of bedforms

The tardy time-adaptation of large bedforms in transient conditions leads to a mismatch between observed bedform shape (and hence identification) and size and the conditions in which they were formed. Small bedforms adapt quickly to changing conditions, typically with tens of minutes (e.g. Traykovski et al., 1999). They may show hysteresis in changing wave energy or direction. Large bedforms adapt slowly (e.g. Allen, 1976), and very large bedforms may not adapt at all but become relics. For example, hummocks and sandwaves on the shelf and dunes on a dry intertidal shoal may have become too large to be destroyed in the waning storm or falling tide. They become relics that are slowly reworked by low-energy conditions or benthic activity or are reactivated in new storms.

Bedforms adapt by redistribution of sediment. The time-scale of adaptation can therefore be estimated by the bedform volume normalised with near-bed sediment transport rate (Allen, 1976). Theoretically an exponential decline in adaptation is expected due to decreasing sediment transport gradients in the process of adaptation. 63% of the adaptation is done in the time estimated from the initial sediment transport rate. This was experimentally confirmed for current dunes (Allen, 1976), tidal dunes (Allen and Friend, 1976) and current ripples (Baas, 1994, 1999). Similar approaches were applied to wave ripples but were less successful (Vongvissensomjai et al., 1986). When the new ripple wavelength is an harmonic of the old, then the adaptation is expected to be more complex. Doucette and O'Donoghue (pers. comm.) found a shear-stress independent time-adaptation of wave ripples to step-wise changes.

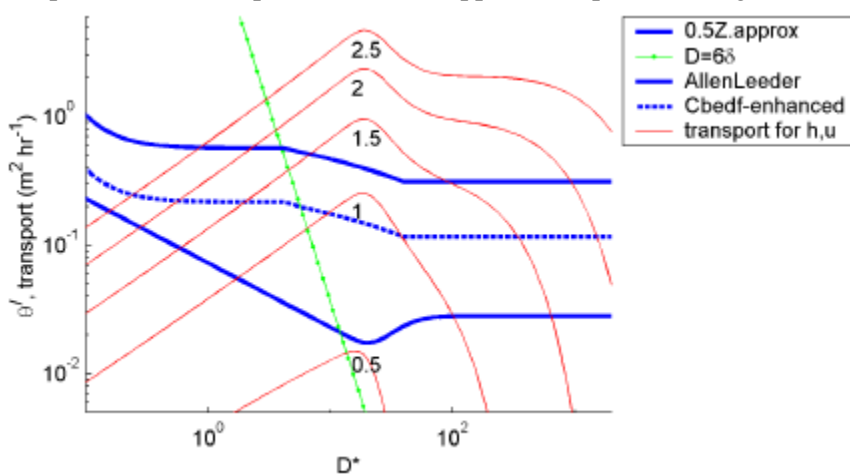


Figure 9 Sediment transport ($m^3 m^{-1} hour^{-1}$) for 3 m water depth and various velocities (numbers, $m s^{-1}$).

The relevant sediment transport component is best estimated by bedform celerity but this quantity is rarely available. A first-order approximation is therefore given by a bedload sediment transport predictor

(Ribberink, 1998, Kleinhans, this volume) or by flow velocity to the power of 3-5. The time-scale of adaptation can be estimated for different bedform sizes (Figure 9). For example, a velocity of 1 m s^{-1} in 3 m water depth at $D^*=15$ gives about $0.2 \text{ m}^2 \text{ hour}^{-1}$ of transport. A triangular bedform of 0.1 m high and 1 m long contains 0.1 m^2 of sediment, which is removed in about an hour. For a velocity of 0.5 m s^{-1} the transport rate is a factor of 10 smaller which increases the time-scale of adaptation with the same factor.

5.4 Consequences for bedform dimension predictors

Bedform dimension models commonly predict that heights approximate zero at incipient motion and near sheetflow. Many predictors were shown, however, to be based on sheetflow criteria that are inconsistent with logical and empirical arguments. Others, like the wave ripple steepness predictor of Nielsen, assume a constant Shields number for sheet flow, which conflicts with the present proposal. For bedform height or steepness predictors to be testable (and potentially valid) for a large range of grain size, they must have a format incorporating the incipient motion and sheetflow criteria, similar to Van Rijn (1984, in 1993):

$$(\eta \text{ or } \eta/\lambda) = f[(\theta_i - \theta_{cr}), (\theta_{sh} - \theta_i), K \tan \psi] \quad (21)$$

such that sediment mobility is indicated by $(\theta_i - \theta_{cr})$ with, e.g., the Zanke model, bedforms disappear when $(\theta_{sh} - \theta_i) < 0$ for, e.g., the Allen-Leeder model, and steepness never exceeds the angle of repose $\tan \psi$ (corrected for cohesion). The bedform length may also depend on other parameters such as grain size.

Finally, despite decades of effort there still is a lack of data on activity of large ($\lambda > 5 \text{ m}$) bedforms during storms, bedforms in combined currents and waves with various angles, and on bed states (including sheet flow) in coarse sand, gravel and mixtures under waves. Such data are badly needed for testing the new diagrams and extend the grain-size validity range for bed state predictors.

6 CONCLUSIONS

Existing bed state stability diagrams and bedform predictors show spectacular disagreements when extended to grain sizes beyond 0.1-0.5 mm, but also striking similarities with rational criteria for transitions between bed states. A set of new phase diagrams for bed states in currents, waves and combined flows is based on nondimensional grain shear stress for currents and waves and on nondimensional grain size. The transitions between bed states are defined by rational criteria for incipient motion, sheetflow and hydraulic smooth/rough flow. For the combined flow diagram a normalisation for grain size allows plotting with two variables only. Earlier diagrams and recent combined flow data collapse well on the rational transitions of the new diagrams, demonstrating their empirical validity for grain sizes of 0.04-40 mm and bed states from no motion to above sheetflow. In addition, the diagrams are a modular framework in which alternative threshold and transition functions can be plotted. The diagrams suggest a format for bedform dimension predictors.

7 REFERENCES

- Allen, J. R. L., 1976.** Computational models for dune time-lag: general ideas, difficulties, and early results. *Sedimentary Geology* 15, 1-53.
- Allen, J. R. L., 1984.** Sedimentary structures, their character and physical basis. *Developments in Sedimentology* 30, I and II, Elsevier, Amsterdam, The Netherlands.
- Allen J. R. L. and Friend, P. F., 1976.** Relaxation time of dunes in decelerating aqueous flows. *J. Geol. Soc. London* 132, 17-26.
- Allen J. R. L. and Leeder, M. R., 1980.** Criteria for the instability of upper-stage plane beds. *Sedimentology* 27, 209-217.
- Amos, C. L., Bowen, A. J., Huntley, D. A. and Lewis, C. F. M., 1988.** Ripple generation under the combined influences of waves and currents on the Canadian continental shelf. *Continental Shelf Research* 8 (10), 1129-1153.
- Amos, C.L., Li, M. Z. and Choung, K.-S., 1996.** Storm-generated, hummocky cross-stratification on the outer-Scotian shelf. *Geo-Marine Letters* 16, 85-94.
- Ardhuin, F., Drake, T. G. and Herbers, T. H. C., 2002.** Observations of wave-generated vortex ripples on the North Carolina continental shelf. *J. Geophysical Research* 107 (C10), 3143, doi:10.1029/2001JC000986.
- Arnott, R. W. and Southard, J. B., 1990.** Exploratory flow-duct experiments on combined-flow bed configurations, and some implications for interpreting storm-event stratification. *Journal of Sedimentary Petrology* 60, 211-219.

- Ashley, G. M. 1990.** Classification of large-scale subaqueous bedforms: a new look at an old problem. *J. of Sedimentary Petrology* 60(1), 160-172.
- Baas, J.H., 1994.** A flume study of the development and equilibrium morphology of current ripples in very fine sand. *Sedimentology* 41, 185-209.
- Baas, J.H., 1999.** An empirical model for the development and equilibrium morphology of current ripples in fine sand. *Sedimentology* 46, 123-138.
- Baas, J.H. and de Koning, H. 1995.** Washed-out ripples: their equilibrium dimensions, migration rate, and relation to suspended-sediment concentration in very fine sand. *J. of Sedimentary Research* A65(2), 431-435.
- Bridge, J.S., 1981.** Bed shear stress over subaqueous dunes, and the transition to upper-stage plane beds. *Sedimentology* 28, 33-36.
- Buffington, J. M. and Montgomery, D. R., 1997.** A systematic analysis of eight decades of incipient motion studies, with special reference to gravel-bedded rivers. *Water Resources Research* 33 (8), 1993-2029.
- Buffington, J. M. and Montgomery, D. R., 1998.** Correction to "A systematic analysis of eight decades of incipient motion studies, with special reference to gravel-bedded rivers". *Water Resources Research* 34 (1), 157.
- Carling, P.A., 1999.** Subaqueous gravel dunes. *Journal of Sedimentary Research* 69, 534-545.
- Davies, T.R.H., 1982.** Discussion of Bridge 1981 (and reply by Bridge). *Sedimentology* 29, 743-747.
- Dinehart, R.L., 1992.** Evolution of coarse gravel bed forms: field measurements at flood stage. *Water Resources Research* 28, 2667-2689.
- Forbes, D. L. and Boyd, R., 1987.** Gravel ripples on the inner Scotian shelf. *J. of Sedimentary Petrology* 57(1), 46-54
- Grant, W. D. and Madsen, O. S., 1982.** Movable bed roughness in unsteady oscillatory flow. *J. of Geophysical Research* 87(C1), 469-481.
- Grasmeijer, B. T. and Kleinhans, M. G. 2004.** Observed and predicted bed forms and their effect on suspended sand concentrations. *Coastal Engineering* 51, 351-371.
- Green, M. O. 1999.** Test of sediment initial-motion theories using irregular-wave field data. *Sedimentology* 46, 427-441.
- Hanes, D. M., Alymov, V. and Chang, Y. S., 2001.** Wave-formed sand ripples at Duck, North Carolina. *Journal of Geophysical Research* 106 (C10), 22575-22592.
- Julien, P. Y. and Raslan, Y., 1998.** Upper-regime plane bed. *J. of Hydraulic Engineering* 124(11), 1086-1096.
- Kleinhans, M. G., Wilbers, A. W. E., De Swaaf, A. and Van den Berg, J. H., 2002.** Sediment supply-limited bedforms in sand-gravel bed rivers. *J. of Sedimentary Research* 72(5), 629-640.
- Komar, P. D. and Miller, M. C., 1975.** The initiation of oscillatory ripple marks and the development of plane-bed at high shear stresses under waves. *J. of Sedimentary Petrology* 45(3), 697-703.
- Li, M. Z. and Amos, C. L., 1999a.** Sheet flow and large wave ripples under combined waves and currents: field observations, model predictions and effects on boundary layer dynamics. *Continental Shelf Research* 19, 637-663.
- Li, M. Z. and Amos, C. L., 1999b.** Field observations of bedforms and sediment transport thresholds of fine sand under combined waves and currents. *Marine Geology* 158, 147-160.
- Myrow, P. M. and Southard, J. B. 1991.** Combined-flow model for vertical stratification sequences in shallow marine storm-deposited beds. *J. of Sedimentary Research* 61 (2), 202-210.
- Nielsen, P., 1981.** Dynamics and geometry of wave-generated ripples. *J. of Geophysical Research* 86(C7), 6467-6472.
- Nielsen, P., 1992.** Coastal bottom boundary layers and sediment transport. *Advanced Series on Ocean Engineering* 4, World Scientific, Singapore, 324.
- Parker, G. in prep.** Transport of gravel and sediment mixtures. In: *ASCE Manual 54, Sedimentation Engineering*, Garcia, M. in prep. (ed.), draft on <http://www.ce.umn.edu/~parker/>.
- Ribberink, J. S., 1995.** Time-averaged sediment transport phenomena in combined wave-current flows. Part II, Report H1889.11, Delft Hydraulics, Delft, The Netherlands.
- Ribberink, J. S. and Al-Salem, A. A., 1994.** Sediment transport in oscillatory boundary layers in cases of rippled beds and sheet flow. *J. of Geophysical Research* 99(C6), 12707-12727.
- Simons, D.B., and Richardson, E.V., 1965.** A study of variables affecting flow characteristics and sediment transport in alluvial channels. In: *Federal Inter-Agency Sediment Conference 1963 Proceedings: US Department of Agriculture publication 970*, 193-207.
- Soulsby, R. 1987.** Calculating bottom orbital velocity beneath waves. *Coastal Engineering* 11, 371-380.
- Soulsby, R. 1997.** *Dynamics of marine sands*. Thomas Telford Publications, London, United Kingdom.

- Southard, J. B. and Boguchwal, A.L., 1990.** Bed configurations in steady unidirectional water flows. Part 2. Synthesis of flume data: *Journal of Sedimentary Petrology* 60, 658-679.
- Southard, J. B., Lambi , J. M., Federico, D. C., Pile, H. T. and Weidman, C. R., 1990.** Experiments on bed configurations in fine sands under bidirectional purely oscillatory flow, and the origin of hummocky cross-stratification. *Journal of Sedimentary Petrology* 60, 1-17.
- Sternberg, R. W. and Larsen, L. H., 1975.** Threshold of sediment movement by open ocean waves: observations. *Deep-Sea Research* 22, 299-309.
- Swift et al 1983
- Traykovski, P., Hay, A. E., Irish, J. D. and Lynch, J. F., 1999.** Geometry, migration, and evolution of wave orbital ripples at LEO-15. *Journal of Geophysical Research* 104 (C1), 1505-1524.
- Van de Meene, J. W. H., Boersma, J. R. and Terwindt, J. H. J., 1996.** Sedimentary structures of combined flow deposits from the shoreface-connected ridges along the central Dutch coast. *Marine Geology* 131, 151-175.
- Van den Berg, J.H. and Van Gelder, A., 1993.** A new bedform stability diagram, with emphasis on the transition of ripples to plane bed in flows over fine sand and silt: *Special Publications of the International Association of Sedimentologists* 17, 11-21.
- Van Rijn, L.C. 1984.** Sediment transport, part I: bed load transport, *J.of Hydraul. Eng.* 110(10), 1431-1456.
- Van Rijn, L. C., 1993.** Principles of sediment transport in rivers, estuaries and coastal seas, Aqua Publications, Oldemarkt, The Netherlands.
- Vongvisessomjai, S., Munasinghe, L. C. J. and Gunaratna, P. P., 1986.** Transient ripple formation and sediment transport. *Coastal Engineering conference*, 1638-1652.
- Wiberg, P. L. and Smith, J. D., 1987.** Calculations of the critical shear stress for motion of uniform and heterogeneous sediments. *Water Resources Research* 23(8), 1471-1480.
- Wilbers, A., 2004.** The development and hydraulic roughness of subaqueous dunes. *Netherlands Geographical Studies* 323 (PhD-thesis), The Royal Dutch Geographical Society, Faculty of Geosciences, Utrecht University, The Netherlands, 227 pages.
- Wilson, K. C., Andersen, J. S. and Shaw, J. K., 1995.** Effects of wave asymmetry on sheet flow. *Coastal Engineering* 25, 191-204.
- Zanke, U.C.E. 2003.** On the influence of turbulence on the initiation of sediment motion, *International J. of Sediment Research* 18(1), 1-15.

8 ACKNOWLEDGEMENTS

I thank Tom O'Donoghue and Jeff Doucette for their hospitality and discussion over their fresh flow tunnel experiments on (transient) ripples during my three-week stay at Aberdeen University. For discussion I thank Bart Grasmeyer, Janrik van den Berg, Tony Dolphin, Jan Ribberink, Jebbe van de Werf, Aart Kroon, Pim van Santen, Dick Mastbergen, Gerard Kruse, Richard Soulsby, Karl Eidsvik, Dag Myrhaug, Enrico Foti and Leo van Rijn. The research was funded by EC MAST, MAS3--CT97--0086